

Journal Pre-proofs

Research paper

Using thiol-amine solvent mixture to prepare main group heterometallic chalcogenides

Ji-Ming Yu, Ting Cai, Zhong-Jie Ma, Fei Wang, Huan Wang, Ji-Peng Yu, Lu-Lu Xiao, Fang-Fang Cheng, Wei-Wei Xiong

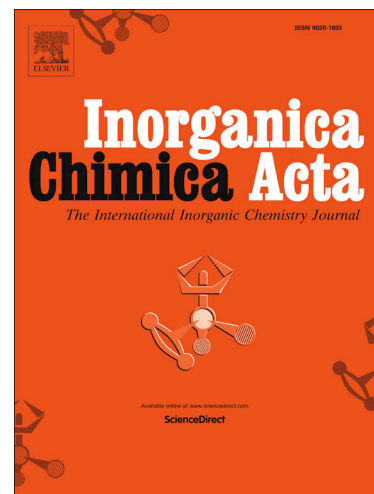
PII: S0020-1693(19)31879-1
DOI: <https://doi.org/10.1016/j.ica.2020.119697>
Reference: ICA 119697

To appear in: *Inorganica Chimica Acta*

Received Date: 1 December 2019
Revised Date: 18 April 2020
Accepted Date: 22 April 2020

Please cite this article as: J-M. Yu, T. Cai, Z-J. Ma, F. Wang, H. Wang, J-P. Yu, L-L. Xiao, F-F. Cheng, W-W. Xiong, Using thiol-amine solvent mixture to prepare main group heterometallic chalcogenides, *Inorganica Chimica Acta* (2020), doi: <https://doi.org/10.1016/j.ica.2020.119697>

This is a PDF file of an article that has undergone enhancements after acceptance, such as the addition of a cover page and metadata, and formatting for readability, but it is not yet the definitive version of record. This version will undergo additional copyediting, typesetting and review before it is published in its final form, but we are providing this version to give early visibility of the article. Please note that, during the production process, errors may be discovered which could affect the content, and all legal disclaimers that apply to the journal pertain.



Title Page

Title: Using thiol-amine solvent mixture to prepare main group heterometallic chalcogenides

Authors: Ji-Ming Yu^a, Ting Cai^a, Zhong-Jie Ma^a, Fei Wang^a, Huan Wang^a, Ji-Peng Yu^a, Lu-Lu Xiao^a, Fang-Fang Cheng^{b,*}, Wei-Wei Xiong^{a,*}

Affiliation: ^aKey Laboratory of Flexible Electronics (KLOFE) & Institute of Advanced Materials (IAM), Jiangsu National Synergetic Innovation Center for Advanced Materials (SICAM), Nanjing Tech University (NanjingTech), 30 South Puzhu Road, Nanjing 211816, P.R. China.

^bSchool of Pharmacy, Nanjing University of Chinese Medicine, Nanjing 210023, P.R. China.

*Corresponding author:

Wei-Wei Xiong

Key Laboratory of Flexible Electronics (KLOFE) & Institute of Advanced Materials (IAM), Jiangsu National Synergetic Innovation Center for Advanced Materials (SICAM), Nanjing Tech University (NanjingTech), 30 South Puzhu Road, Nanjing 211816, P.R. China.

Tel: (+65) 18951703763.

E-mail: iamwwxiong@njtech.edu.cn

Fang-Fang Cheng

School of Pharmacy, Nanjing University of Chinese Medicine, Nanjing 210023, P.R. China.

Tel: (+65) 15051848528.

E-mail: ffcheng@njucm.edu.cn

Using thiol-amine solvent mixture to prepare main group heterometallic chalcogenides

Ji-Ming Yu^a, Ting Cai^a, Zhong-Jie Ma^a, Fei Wang^a, Huan Wang^a, Ji-Peng Yu^a, Lu-Lu Xiao^a,
Fang-Fang Cheng^{b,*}, Wei-Wei Xiong^{a,*}

^aKey Laboratory of Flexible Electronics (KLOFE) & Institute of Advanced Materials (IAM), Jiangsu National Synergetic Innovation Center for Advanced Materials (SICAM), Nanjing Tech University (NanjingTech), 30 South Puzhu Road, Nanjing 211816, P.R. China.

^bSchool of Pharmacy, Nanjing University of Chinese Medicine, Nanjing 210023, P.R. China.

Abstract

By using a n-butylamine (BA)-1,2-ethanedithiol (EDT) solvent mixture as reaction medium, three new heterometallic chalcogenides have been prepared, namely $[\text{HBA}]_{2.6}[\text{In}_{2.6}\text{Sn}_{1.4}\text{Se}_6\text{S}_2]$ (**1**), $[\text{HBA}]_{0.8}[\text{HR-MP}]_2[\text{In}_{2.8}\text{Sn}_{1.2}\text{Se}_6\text{S}_2]$ (**2**) ($R\text{-MP} = (R)\text{-2-methylpiperazines}$) and $[\text{H}_3\text{TAEA}]_2[\text{InGe}_4\text{S}_{11}(\text{SH})_2(\text{OH})]$ (**3**) (TAEA = tris(2-aminoethyl)amine). Compounds **1** and **2** feature anionic two-dimensional $[\text{In}_x\text{Sn}_{4-x}\text{Se}_6\text{S}_2]^{x-}$ layers built up by $[\text{M}_4\text{Q}_{10}]$ ($\text{M} = \text{In/Sn}$, $\text{Q} = \text{Se/S}$) T2 clusters. Protonated HBA^+ and HR-MP^+ cations serve as charge balance agents located between the layers. Compound **3** contains discrete $[\text{InGe}_4\text{S}_{11}(\text{SH})_2(\text{OH})]^{6-}$ anionic clusters, in which the In^{3+} ion adopts a unique penta-coordination geometry with five S^{2-} ions. These compounds were characterized by single crystal X-ray diffraction, powder X-ray diffraction, energy dispersive X-ray spectroscopy, solid-state UV-Vis diffuse reflectance spectroscopy, and thermogravimetric analyses. The steep UV-Vis absorption edges indicate the band gaps of 1.86 eV for **1**, 2.13 eV for **2** and 2.78 eV for **3**.

Keywords: Thiol-amine solvent mixture; Heterometallic chalcogenides; Crystal structure; Photocatalysis.

* Corresponding author. Tel: (+65) 18951703763. E-mail: iamwwxiong@njtech.edu.cn

1. Introduction

Crystalline metal chalcogenides exhibit prominent performances in the areas of ion exchange [1-4], thermoelectricity [5-8], photoelectric catalysis [9-15], and electrochemical energy storage [16-19]. The structure and component of these materials play a dominant role in determining their properties, while the participation of main group metals offer more possibilities for harvesting diverse topologies [20-26]. Generally, the most preferable coordination mode between group 13/14 metals and chalcogen atoms is tetrahedral coordination geometry [27-30]. Four such tetrahedrons could set up a supertetrahedral T2 cluster (e.g. $[\text{Ga}_4\text{Q}_{10}]^{8-}$, $[\text{In}_4\text{Q}_{10}]^{8-}$ [31], $[\text{Ge}_4\text{Q}_{10}]^{4+}$ [32,33], $[\text{Sn}_4\text{Q}_{10}]^{4+}$ [34], Q = S, Se). The variable connection style between these T2 clusters can produce different structures [27,35]. Metal chalcogenides built up by supertetrahedral clusters are usually synthesized in conventional solvents, such as water, methanol, DMF, and acetonitrile [36-39]. However, binary intermediate phases (In_2S_3 , In_2Se_3 , GeS, SnS, SnSe) are usually generated as byproducts in the reaction process, and their low solubility in the conventional solvents could consume the metal and chalcogen ions via precipitation, which hinders the reaction process to construct complex frameworks. Hence, in order to prevent the binary intermediate phases from precipitating in the reaction process, applying new type of reaction media possessing high solubility to the binary intermediate phases is unprecedented.

To solve the insolubility of binary chalcogenides in the conventional solvents, Mitzi and co-workers utilized the reducing power of hydrazine to dissolve bulk binary chalcogenides in an excess of elemental chalcogen at room temperature [40-44]. Owing to the outstanding solubility of hydrazine for binary chalcogenides, hydrazine has been used to dissolve various bulk chalcogenides to form homogeneous solutions, which facilitate the deposition of chalcogenide thin films [41,42,45]. However, the high toxicity and explosion hazard of hydrazine limit its wide application in the fabrication of chalcogenide devices. In recent years, Brutchey *et al.* reported a binary alkali system consisting of thiol and amine solvents, which exhibited excellent solubility for a variety of bulk binary

chalcogenides, such as In_2S_3 , In_2Se_3 , SnS , and SnSe [46-51]. These thiol-amine solvent mixtures facilitated the spin coating process of metal chalcogenide thin films, and further promoted the application of bulk binary chalcogenides in photovoltaic conversion [52-56]. In contrast to hydrazine, the thiol-amine solvent mixtures are much safer and less toxic. Moreover, this alkaline system could dissolve diverse elemental main group metals and its oxides at room temperature. Besides, diversiform combinations of thiol-amine mixture provide more choices for varying the reaction environment. Additionally, the strong solubility of thiol-amine solvent mixtures may forbid the precipitation of the as-formed binary intermediate phases from reaction systems and promote the setup of new frameworks. Until recently, we have used this thiol-amine solvent system to prepare a series of new chalcogenidoarsenates [57], and thus more efforts are required to put into this research area.

On the basis of this motivation, we actively tried to employ this thiol-amine solvent system in the synthesis of crystalline metal chalcogenides based on group 13 and 14 metals. In this work, by using monoamine/dithiol solvent mixture (vol/vol = 1:1 of n-butylamine/1,2-ethanedithiol) as reaction medium, we synthesized three new heterometallic chalcogenides, namely, $[\text{HBA}]_{2.6}[\text{In}_{2.6}\text{Sn}_{1.4}\text{Se}_6\text{S}_2]$ (**1**), $[\text{HBA}]_{0.8}[\text{HR-MP}]_2[\text{In}_{2.8}\text{Sn}_{1.2}\text{Se}_6\text{S}_2]$ (**2**), and $[\text{H}_3\text{TAEA}]_2[\text{InGe}_4\text{S}_{11}(\text{SH})_2(\text{OH})]$ (**3**). Compounds **1** and **2** contain the similar 2D anionic layers $[\text{In}_x\text{Sn}_{4-x}\text{Se}_6\text{S}_2]^{x-}$ separated by protonated n-butylamine cations and (*R*)-2-methylpiperazine cations. Compound **3** is composed of anionic discrete $[\text{InGe}_4\text{S}_{11}(\text{SH})_2(\text{OH})]^{6-}$ clusters. The In^{3+} ion in **3** exhibits a penta-coordination geometry, which is unusual in the reported indium sulfides. It should be noted that no crystals can be obtained when replacing the BA-EDT solvent mixture with other conventional solvents. The photocatalytic activity of compound **1** for degrading RhB was investigated.

2. Experimental section

2.1. Materials and general methods

All reagents and chemicals were purchased from commercial sources as analytical grade and without further purification. Elemental analyses of C, H, N and S were carried out on a German Elementary Vario EL III instrument. The mapping analyses of In, Sn, Ge, S and Se have been performed on a JEOL JSM-7800F scanning electron microscope. Powder X-ray diffraction (PXRD) patterns were recorded in the angular range of $2\theta = 5-65^\circ$ on a Rigaku Mini-Flex II diffractometer using $\text{CuK}\alpha$ radiation. Optical diffuse reflectance spectra were measured at room temperature with an UV-vis-NIR Varian 86 Cary 500 Scan spectrophotometer using a BaSO_4 plate as a standard (100% reflectance). The absorption (α/S) data were calculated from reflectance spectra by using the Kubelka–Munk function: $\alpha/S = (1 - R)^2/2R$, where α is the absorption coefficient, S is the scattering coefficient, and R is the reflectance. The thermogravimetric analyzer was performed on a NETZSCH DSC214Polyma instrument under flowing N_2 with a heating rate of $10^\circ\text{C}/\text{min}$ in the temperature range of $30-800^\circ\text{C}$.

2.2. Synthesis

Synthesis of $[\text{HBA}]_{2.6}[\text{In}_{2.6}\text{Sn}_{1.4}\text{Se}_6\text{S}_2]$ (**1**). $\text{In}(\text{NO}_3)_3 \cdot \text{H}_2\text{O}$ (0.96 mmol, 0.306 g), Sn (1.01 mmol, 0.120 g), Se (6.27 mmol, 0.495 g), 1,8-diaminooctane (3.54 mmol, 0.511 g) and n-butylamine/1,2-ethanedithiol (3 mL, vol/vol = 1:1) were mixed and sealed in an autoclave equipped with a Teflon liner (20 mL), then heated at 160°C for 5 days and cooled to room temperature. The products were filtrated and washed several times with ethanol to obtain orange flake crystals of **1** with a yield of 46.5% (based on In). Anal. calc. for **1** : C, 10.45%; H, 2.63%; N, 3.04%; S, 5.36%. Found : C, 10.69%; H, 2.48%; N, 3.24%; S, 4.39%.

Synthesis of $[\text{HBA}]_{0.8}[\text{HR-MP}]_2[\text{In}_{2.8}\text{Sn}_{1.2}\text{Se}_6\text{S}_2]$ (**2**). $\text{In}(\text{NO}_3)_3 \cdot \text{H}_2\text{O}$ (0.94 mmol, 0.301 g), Sn (0.66 mmol, 0.078 g), Se (4.03 mmol, 0.318 g), (*R*)-2-methylpiperazine (2.06 mmol, 0.206 g) and n-butylamine/1,2-ethanedithiol (3 mL, vol/vol = 1:1) were mixed and sealed in an autoclave equipped with a Teflon liner (20 mL), then heated at 160°C for 5 days and cooled to room temperature. The products were filtrated and washed several times with ethanol to obtain yellow needle crystals of **2**

with a yield of 23.6% (based on In). Anal. calc. for **2** : C, 12.55%; H, 2.84%; N, 5.32%; S, 5.08%; Found : C, 12.08%; H, 2.60%; N, 5.18%; S, 5.03%.

Synthesis of $[\text{H}_3\text{TAEA}]_2[\text{InGe}_4\text{S}_{11}(\text{SH})_2(\text{OH})]$ (**3**). $\text{In}(\text{NO}_3)_3 \cdot \text{H}_2\text{O}$ (0.93 mmol, 0.298 g), GeO_2 (1.02 mmol, 0.107 g), S (5.22 mmol, 0.167 g), tris(2-aminoethyl)amine (3.49 mmol, 0.511 g), ethylene glycol (1 mL) and n-butylamine/1,2-ethanedithiol (3 mL, vol/vol = 1:1) were mixed and sealed in an autoclave equipped with a Teflon liner (20 mL), then heated at 170 °C for 5 days and cooled to room temperature. The products were filtrated and washed several times with ethanol to obtain pale yellow block crystals of **3** with a yield of 44.3% (based on In). Anal. calc. for **3**: C, 12.65%; H, 3.98%; N, 9.83%. Found : C, 13.13%; H, 3.66%; N, 9.73%.

2.3. Single-crystal structure determination

Single-crystal X-ray diffraction data of compounds **1-3** were collected on a Xcalibur Eos CCD diffractometer with graphite-monochromated $\text{MoK}\alpha$ radiation ($\lambda = 0.71073 \text{ \AA}$) at room temperature. The absorption corrections were determined using a multi-scan technique. The structures of **1-3** were analyzed by direct methods and refined by full-matrix least-squares on F^2 using the SHELX-2016 program package [58]. In the structure of compound **1**, the protonated n-butylamine cations are highly disordered and could not be recognized from the difference-Fourier map. Thus, the SQUEEZE routine of PLATON program was used to dismiss the scattering from the cations. The structural formulas of compounds **1** and **2** were determined with the aid of elemental analysis and EDX data. Crystallographic data and structural refinements are summarized in Table 1. The mapping images for compounds **1-3** are showed in Figure 1.

2.4. Photocatalytic activity measurement

30 mg of **1** was suspended in 50 mL aqueous solution of Rhodamine B (RhB, 10 mg/L), and the mixture was stirred in darkness for 30 min to reach the adsorption/desorption equilibrium between the

catalyst and RhB. Then the mixture was exposed to visible light irradiation using a 300 W xenon lamp equipped with filter ($\lambda > 420$ nm). 3 mL of the suspension was taken from the mixture for each 30 min, and the catalysts were separated by centrifugation, and then the remained solution was tested by UV-vis spectrum. Degradation efficiency was judged by C/C_0 , C was the instant RhB concentration while C_0 was the initial concentration of RhB [59].

3. Results and discussion

Compounds **1-3** are heterometallic chalcogenides based on group 13 (In) and 14 (Ge, Sn) metals. Crystals of **1** and **2** were obtained by reacting $\text{In}(\text{NO}_3)_3 \cdot \text{H}_2\text{O}$, Sn and Se with different organic ligands in BA-EDT solvent mixture at 160 °C. In the synthesis of **1**, the protonated n-butylamine cations rather than 1,8-diaminooctane acted as charge balance agent, since crystals of **1** with low yield and bad quality can be prepared by replacing 1,8-diaminooctane with other nitrogen donor ligands or surfactants, such as 1,12-dodecanediamine, 1,2-diaminocyclohexane, pyridine, 1,5-diazabicyclo[4.3.0]non-5-ene (DBN), octyltrimethylammonium chloride, 1-hexanol, *et al.* However, compared with other nitrogen donor ligands, the crystals prepared in the present of 1,8-diaminooctane were in high yield and good quality. Therefore, performing as an auxiliary reagent, surfactant 1,8-diaminooctane was beneficial for crystal growth [60-62]. Obviously, nitrogen donor ligands play a crucial role in the crystal growth, although some of them did not serve as charge balance agents [63-65]. Compound **3** was synthesized by reacting $\text{In}(\text{NO}_3)_3 \cdot \text{H}_2\text{O}$, GeO_2 , S, tris(2-aminoethyl)amine and ethylene glycol in BA-EDT solvent mixture. It was worth noting that ethylene glycol was indispensable during the reaction process of **3**. As an important auxiliary solvent, ethylene glycol was conducive to the crystal growth of **3**, because no crystals can be harvested by removing ethylene glycol from the reaction system (Scheme 1). We have investigated the effect of reaction temperature to the syntheses of these compounds. The most suitable reaction temperature for the crystal growth of **1** and **2** was 160 °C, while higher (170 °C, 180 °C) or lower (150 °C)

temperature could produce crystals with lower yields and bad quality. In the synthesis of compound **3**, when the reaction temperature was 150 °C, only unknown white powder was obtained; when the reaction temperature was increased to 180 °C, crystals of **3** with bad quality were obtained. Thus, 170 °C was the most suitable temperature for the crystal growth of **3**.

Aim to investigate the significant role of thiol-amine solvent mixture in the synthesis of compounds **1-3**, some conventional solvents such as water, methanol and acetonitrile were used to substitute the BA-EDT solvent mixture. However, no crystals could be obtained. Further experiments showed that when removing or replacing one of components from the binary solvent system, such as replacing BA with ethylenediamine or ethanolamine, EDT with ethanethiol or propanethiol, no target products can be formed as well. Accordingly, BA-EDT solvent mixture is the most suitable solvent system for the preparation of compounds **1-3**. Compounds **1** and **2** were synthesized by heating the starting materials at 160 °C. This reaction environment could promote the decomposition of 1,2-ethanedithiol, and thus S²⁻ ions were produced to take part in the assembly of the frameworks of **1** and **2**.

Single crystal X-ray analysis indicates that [HBA]_{2.6}[In_{2.6}Sn_{1.4}Se₆S₂] (**1**) crystallizes in the tetragonal space group *P4₂/nmc* and contains two-dimensional anionic layers [In_{2.6}Sn_{1.4}Se₆S₂]_n^{2.6n-}. In the anionic layer of **1**, the In and Sn atoms could not be differentiated by crystallographic analysis. Similar case is encountered for distinguishing the Se and S atoms. Based on the elemental analysis and EDX results (Figure S4), all the metal sites are assigned to the co-occupied In and Sn atoms with a ratio of 0.65/0.35, while all the chalcogen sites are assigned to the co-occupied Se and S atoms with a ratio of 0.75/0.25. Each In³⁺/Sn⁴⁺ ion tetrahedrally coordinates with four Q²⁻ ions to build a [MQ₄] tetrahedron (M = In/Sn, Q = Se/S). Four [MQ₄] tetrahedrons are connected with each other via corner-sharing Q atoms to set up a [M₄Q₁₀] T2 cluster subunit. These subunits extend by means of corner-sharing connection to construct a [In_{2.6}Sn_{1.4}Se₆S₂]_n^{2.6n-} layer (Fig. 2a), in which the protonated n-butylamine cations are supposed to locate between the layers as charge balance agents (Fig. 2b). The

$[\text{In}_{2.6}\text{Sn}_{1.4}\text{Se}_6\text{S}_2]_n^{2.6n-}$ layer of **1** contains windows formed by four T2 clusters with a dimension of $7.8715 \times 7.8715 \text{ \AA}$. The adjacent layers have inverse configurations arranged in the *ab*-plane along the *c*-axis, which is isostructural to CsGaTe_2 , CsInSe_2 , KInS_2 and so on [66-68]. The M-Q bond lengths of **1** vary from 2.509(3) to 2.535(5) \AA , and the M-Q-M angles range from $101.8(3)^\circ$ to $112.71(9)^\circ$.

Compound **2** $[\text{HBA}]_{0.8}[\text{HR-MP}]_2[\text{In}_{2.8}\text{Sn}_{1.2}\text{Se}_6\text{S}_2]$ crystallizes in the orthorhombic space group $Pna2_1$ and contains anionic $[\text{In}_{2.8}\text{Sn}_{1.2}\text{Se}_6\text{S}_2]_n^{2.8n-}$ layers, protonated butylamine cations and (*R*)-2-methylpiperazine cations. Similarly to compound **1**, the In/Sn and Se/S atoms in the anionic layer of **2** could not be distinguished from the difference-Fourier map. According to the elemental analysis and EDX results (Figure S5), the metal and chalcogen sites are assigned to the co-occupied In/Sn and Se/S atoms with ratios of 0.7/0.3 and 0.75/0.25, respectively. The asymmetric unit of compound **2** contains 4 In/Sn atoms, 8 Se/S atoms, 0.8 protonated butylamine and 2 protonated (*R*)-2-methylpiperazines. Compounds **1** and **2** have the similar $[\text{M}_4\text{Q}_{10}]$ T2 cluster subunit, but with different connection configurations (Fig. 3a). The anionic $[\text{In}_{2.8}\text{Sn}_{1.2}\text{Se}_6\text{S}_2]_n^{2.8n-}$ layer of **2** is build up by alternate connection of two types of chains with the reverse directions (Fig. 2a), both *a* and *b* chains are made up by $[\text{M}_4\text{Q}_{10}]$ T2 clusters, while their connections are arranged in an *abab* order. The adjacent layers exhibit an inverted arrangement along the *b*-axis, where the protonated n-butylamine cations and (*R*)-2-methylpiperazine cations serve as charge balance agents located between the layers (Fig. 3b). The M-Q bond lengths vary from 2.490(8) to 2.598(9) \AA , and the M-Q-M angles range from $95.12(12)$ to $116.68(13)^\circ$. In the structures of compounds **1-2**, the M-Q bond lengths are shorter than the conventional Sn-Se bond lengths [69-70], but longer than the In-S bond lengths [71-72]. This difference may be caused by the co-occupation of the In/Sn and Se/S atoms at the metal and chalcogen sites, respectively.

Compound **3** $[\text{H}_3\text{TAEA}]_2[\text{InGe}_4\text{S}_{11}(\text{SH})_2(\text{OH})]$ crystallizes in the orthorhombic space group $Pnma$ and features discrete $[\text{InGe}_4\text{S}_{11}(\text{SH})_2(\text{OH})]^{6-}$ anionic clusters charge-balanced by protonated

tris(2-aminoethyl)amine cations. In the $[\text{InGe}_4\text{S}_{11}(\text{SH})_2(\text{OH})]^{6-}$ cluster, the In atom adopts a special penta-coordinated mode with five S atoms to build a $[\text{InS}_5]$ unit, and Ge atoms have both tetra-coordinated and penta-coordinated coordination modes. Ge1 and Ge2 atoms are tetrahedrally coordinates with four S atoms to set up $[\text{GeS}_4]$ tetrahedrons. Three $[\text{GeS}_4]$ tetrahedrons coordinate with a $[\text{InS}_5]$ unit via corner-sharing S atoms to constitute a pseudo-T2 cluster $[\text{InGe}_3\text{S}_{11}]^{7-}$. Ge3 atom exhibits a five coordination mode with O and S atoms to build a $[\text{GeS}_2(\text{SH})_2(\text{OH})]^{3-}$ unit, in which the terminal Ge3-S1 and Ge3-S2 bond lengths are 2.228(10) and 2.239 (115) Å, respectively, relatively longer than Ge1-S8 (2.169 Å) and Ge2-S7 (2.179 Å) bond lengths, indicating the presence of (SH)-groups. Finally, the $[\text{GeS}_2(\text{SH})_2(\text{OH})]^{3-}$ is connected with linking units $[\text{InS}_5]$ through edge-sharing to establish a discrete cluster (Fig. 4a). The In-S bond lengths vary from 2.472(5) to 2.630(5) Å, and the S-In-S angles range from 78.9(2) to 146.81(15)°. The Ge-S bond lengths fall in the range of 2.1689(40)-2.239(115) Å, and the S-Ge-S angles range from 105.53(12) to 112.91(12)°.

The solid-state UV-vis diffuse reflectance data of compounds **1-3** were collected at room temperature and converted to optical absorption spectra by using the Kubelka-Munk function method (Fig. 5). The steep absorption edges suggest that the band gaps of **1-3** can be estimated as 1.86 eV, 2.13 eV, and 2.78 eV, respectively, indicating that these compounds are semiconductors.

Thermogravimetric analyses of compounds **1-3** were investigated from 30 °C to 800 °C in a N_2 atmosphere (Fig. 6). Compound **1** exhibited a weight reduction of 21.25% between 30 and 360 °C, which may be attributed to the removal of all n-butylamine cations (16.13%) and two S atoms (5.37%) per formula unit. Compound **2** exhibited a weight loss of 19.50% between 30 and 320 °C owing to the removal of n-butylamine and (*R*)-2-methylpiperazine cations (20.20%), and then a weight decrease of 14.98% between 320 and 800 °C may correspond to the loss of two S atoms (5.11%) and 1.25 Se atoms (9.43%) per formula unit. Compound **3** undergoes a weight loss of 25.80% between 30 to 350 °C corresponding to the release of all tris(2-aminoethyl)amine cations (26.19%), and a weight loss

of 52.24% from 350 to 800 °C may be ascribed to the removal of the one -OH group (1.49%), one S atom (2.81%) and 4 GeS₂ (47.99%) per formula unit.

Photocatalytic activity of compound **1** was evaluated by the degradation of RhB under visible light irradiation ($\lambda > 420$ nm). As shown in Figure 7, the degradation ratio of RhB by **1** reached 98% in 150 min, and achieved nearly complete degradation in 180 min. In contrast, when removing compound **1** from the catalytic reaction, only 19.2% of RhB was degraded in 180 min. Thus, we can conclude that compound **1** is photoactive under visible light irradiation for the degradation of RhB. In addition, the PXRD pattern of **1** after the catalytic reaction was in good agreement with its simulated PXRD pattern from single-crystal XRD data (Fig. S7), indicating the good stability of **1** as photo-catalyst in the degradation process.

4. Conclusions

In summary, we employed a binary solvent mixture of BA and EDT as reaction medium to synthesize of three novel crystalline heterometallic chalcogenides. No crystals could be isolated once the solvent components were replaced by other conventional solvents, indicating the crucial role of the BA-EDT solvent mixture to the crystal growth. Compounds **1** and **2** are characteristic of two dimensional anionic $[\text{In}_x\text{Sn}_{4-x}\text{Se}_6\text{S}_2]^{x-}$ layer with In/Sn and Se/S atoms occupying the same crystallographic position. The protonated n-butylamine cations and (*R*)-2-methylpiperazine cations locate in the interlayer space. Notably, compound **3** features a discrete anionic $[\text{InGe}_4\text{S}_{11}(\text{SH})_2(\text{OH})]^{6-}$ cluster, in which the In³⁺ ion adopts an unusual penta-coordination geometry with five S²⁻ ions. The steep UV-Vis absorption edges of these compounds indicate that they are semiconductors. Compound **1** displayed promising photocatalytic activity for degrading RhB under visible light irradiation. Our explorations proved that the thiol-amine solvent mixtures are promising reaction media for preparing crystalline metal chalcogenides.

Supporting information available

Powder X-ray diffraction patterns, EDX results. CCDC reference numbers 1979504 (1), 1979505 (2), 1979506 (3).

Acknowledgement

W.X acknowledges financial support from National Natural Science Foundation of China (21705081, 21571102), Postgraduate Research & Practice Innovation Program of Jiangsu Province (KYCX19_0859), the Jiangsu Specially-Appointed Professor, “High-Level Talents in Six Industries” of Jiangsu Province (XCL-040).

References

- [1] M.L. Feng, D. Sarma, Y.J. Gao, X.H. Qi, W.A. Li, X.Y. Huang, M.G. Kanatzidis, *J. Am. Chem. Soc.* 140 (2018) 11133-11140.
- [2] X.H. Qi, K.Z. Du, M.L. Feng, Y.J. Gao, X.Y. Huang, M.G. Kanatzidis, *J. Am. Chem. Soc.* 139 (2017) 4314-4317.
- [3] M.L. Feng, D. Sarma, X.H. Qi, K.Z. Du, X.Y. Huang, M.G. Kanatzidis, *J. Am. Chem. Soc.* 138 (2016) 12578-12585.
- [4] M.J. Manos, M.G. Kanatzidis, *J. Am. Chem. Soc.* 131 (2009) 6599-6607.
- [5] J.M. Hodges, S.Q. Hao, J.A. Grovogui, X.M. Zhang, T.P. Bailey, X. Li, Z.H. Gan, Y.Y. Hu, C. Uher, V.P. Dravid, C. Wolverton, M.G. Kanatzidis, *J. Am. Chem. Soc.* 140 (2018) 18115-18123.
- [6] R.G. Deng, X.L. Su, Z. Zheng, W. Liu, Y.G. Yan, Q.J. Zhang, V.P. Dravid, C. Uher, M.G. Kanatzidis, X.F. Tang, *Sci. Adv.* 4 (2018) eaar5606.
- [7] Y.B. Luo, C.F. Du, Q.H. Liang, Y. Zheng, B.B. Zhu, H.L. Hu, K.A. Khor, J.W. Xu, Q.Y. Yan, M.G. Kanatzidis, *Small* 14 (2018) 1803092.
- [8] Y.B. Luo, Y. Zheng, Z.Z. Luo, S.Q. Hao, C.F. Du, Q.H. Liang, Z. Li, K.A. Khor, K. Hippalgaonkar, J.W. Xu, Q.Y. Yan, C. Wolverton, M.G. Kanatzidis, *Adv. Energy Mater.* 8 (2018) 1702167.
- [9] D.L. Liu, Y. Liu, P. Huang, C. Zhu, Z.H. Kang, J. Shu, M.Z. Chen, X. Zhu, J. Guo, L.J. Zhuge, X.H. Bu, P.Y. Feng, T. Wu, *Angew. Chem. -Int. Ed.* 57 (2018) 5374-5378.
- [10] Y.Y. Zhang, D.D. Hu, C.Z. Xue, H.J. Yang, X. Wang, T. Wu, *Dalton Trans.* 47 (2018) 3227-3230.
- [11] Y.Y. Zhang, X. Wang, D.D. Hu, C.Z. Xue, W. Wang, H.J. Yang, D.S. Li, T. Wu, *ACS Appl. Mater. Interfaces* 10 (2018) 13413-13424.
- [12] D.L. Liu, X. Fan, X. Wang, D.D. Hu, C.Z. Xue, Y. Liu, Y. Wang, X. Zhu, J. Guo, H.P. Lin, Y.Y. Li, J. Zhong, D.S. Li, X.H. Bu, P.Y. Feng, T. Wu, *Chem. Mater.* 31 (2019) 553-559.
- [13] L.N. Nie, W.W. Xiong, P.Z. Li, J.Y. Han, G.D. Zhang, S.M. Yin, Y.L. Zhao, R. Xu, Q.C. Zhang, *J. Solid State Chem.* 220 (2014) 118-123.
- [14] L.N. Nie, Q.C. Zhang, *Inorg. Chem. Front.* 4 (2017) 1953-1962.

- [15] Y. Liu, P.D. Kanhere, C.L. Wong, Y.F. Tian, Y.H. Feng, F. Boey, T. Wu, H.Y. Chen, T.J. White, Z. Chen, Q.C. Zhang, *J. Solid State Chem.* 183 (2010) 2644-2649.
- [16] L.N. Nie, J. Xie, G.F. Liu, S.J. Hao, Z.C.J. Xu, R. Xu, Q.C. Zhang, *J. Mater. Chem. A* 5 (2017) 14198-14205.
- [17] L.N. Nie, Y. Zhang, W.W. Xiong, T.T. Lim, R. Xu, Q.Y. Yan, Q.C. Zhang, *Inorg. Chem. Front.* 3 (2016) 111-116.
- [18] J.R. Wang, P. Li, T. Cai, D.D. Yang, W.W. Xiong, *J. Solid State Chem.* 263 (2018) 88-93.
- [19] M. Shao, Y.Y. Cheng, T. Zhang, S. Li, W.N. Zhang, B. Zheng, J.S. Wu, W.W. Xiong, F.W. Huo, J. Lu, *ACS Appl. Mater. Interfaces* 10 (2018) 33097-33104.
- [20] S. Dehnen, M. Melullis, *Coord. Chem. Rev.* 251 (2007) 1259-1280.
- [21] S. Santner, J. Heine, S. Dehnen, *Angew. Chem. -Int. Ed.* 55 (2016) 876-893.
- [22] P.Y. Feng, X.H. Bu, N.F. Zheng, *Acc. Chem. Res.* 38 (2005) 293-303.
- [23] Q.Y. Zhu, J. Dai, *Coord. Chem. Rev.* 330 (2017) 95-109.
- [24] M.G. Kanatzidis, *Inorg. Chem.* 56 (2017) 3158-3173.
- [25] X.F. Xu, W. Wang, D.L. Liu, D.D. Hu, T. Wu, X.H. Bu, P.Y. Feng, *J. Am. Chem. Soc.* 140 (2018) 888-891.
- [26] K.Y. Wang, M.L. Feng, X.Y. Huang, J. Li, *Coord. Chem. Rev.* 322 (2016) 41-68.
- [27] N.F. Zheng, X.G. Bu, B. Wang, P.Y. Feng, *Science* 298 (2002) 2366-2369.
- [28] Y.M. Lin, W. Massa, S. Dehnen, *J. Am. Chem. Soc.* 134 (2012) 4497-4500.
- [29] W.W. Xiong, J.R. Li, B. Hu, B. Tan, R.F. Li, X.Y. Huang, *Chem. Sci.* 3 (2012) 1200-1204.
- [30] Q.C. Zhang, X.H. Bu, Z.E. Lin, M. Biasini, W.P. Beyermann, P.Y. Feng, *Inorg. Chem.* 46 (2007) 7262-7264.
- [31] B. Krebs, D. Voelker, K.O. Stiller, *Inorg. Chim. Acta* 65 (1982) 101-102.
- [32] H. Ahari, A. Garcia, S. Kirkby, G.A. Ozin, D. Young, A.J. Lough, *Dalton Trans.* (1998) 2023-2027.
- [33] K.K. Rangan, P.N. Trikalitis, T. Bakas, M.G. Kanatzidis, *Chem. Commun.* (2001) 809-810.
- [34] A.M. Pirani, H.P.A. Mercier, D.A. Dixon, H. Borrmann, G.J. Schrobilgen, *Inorg. Chem.* 40 (2001) 4823-4829.
- [35] C.F. Du, J.R. Li, B. Zhang, N.N. Shen, X.Y. Huang, *Inorg. Chem.* 54 (2015) 5874-5878.
- [36] Q.C. Zhang, I. Chung, J.I. Jang, J.B. Ketterson, M.G. Kanatzidis, *Chem. Mater.* 21 (2009) 12-14.
- [37] Q.C. Zhang, X.H. Bu, Z.E. Lin, T. Wu, P.Y. Feng, *Inorg. Chem.* 47 (2008) 9724-9726.
- [38] Q.C. Zhang, T. Wu, X.H. Bu, T. Tran, P.Y. Feng, *Chem. Mater.* 20 (2008) 4170-4172.
- [39] Q.C. Zhang, X.H. Bu, J. Zhan, T. Wu, P.Y. Feng, *J. Am. Chem. Soc.* 129 (2007) 8412-8413.
- [40] D.B. Mitzi, L.L. Kosbar, C.E. Murray, M. Copel, A. Afzali, *Nature* 428 (2004) 299-303.
- [41] D.B. Mitzi, M. Copel, S.J. Chey, *Adv. Mater.* 17 (2005) 1285-1289.
- [42] D.J. Milliron, D.B. Mitzi, M. Cope, C.E. Murray, *Chem. Mater.* 18 (2006) 587-590.
- [43] D.B. Mitzi, *Inorg. Chem.* 46 (2007) 926-931.
- [44] D.B. Mitzi, *Adv. Mater.* 21 (2009) 3141-3158.
- [45] D.B. Mitzi, M. Copel, C.E. Murray, *Adv. Mater.* 18 (2006) 2448-2452.
- [46] D.H. Webber, R.L. Brutchey, *J. Am. Chem. Soc.* 135 (2013) 15722-15725.
- [47] J.J. Buckley, M.J. Greaney, R.L. Brutchey, *Chem. Mater.* 26 (2014) 6311-6317.
- [48] D.H. Webber, J.J. Buckley, P.D. Antunez, R.L. Brutchey, *Chem. Sci.* 5 (2014) 2498-2502.
- [49] C.L. McCarthy, D.H. Webber, E.C. Schueller, R.L. Brutchey, *Angew. Chem. -Int. Ed.* 54 (2015) 8378-8381.
- [50] J.J. Buckley, C.L. McCarthy, J. Del Pilar-Albaladejo, G. Rasul, R.L. Brutchey, *Inorg. Chem.* 55 (2016) 3175-3180.
- [51] C.L. McCarthy, R.L. Brutchey, *Chem. Commun.* 53 (2017) 4888-4902.

- [52] Z.Y. Lin, Q.Y. He, A.X. Yin, Y.X. Xu, C. Wang, M.N. Ding, H.C. Cheng, B. Papandrea, Y. Huang, X.F. Duan, *ACS Nano* 9 (2015) 4398-4405.
- [53] F. Liu, J. Zhu, L.H. Hu, B. Zhang, J.X. Yao, M.K. Nazeeruddin, M. Gratzel, S.Y. Dai, *J. Mater. Chem. A* 3 (2015) 6315-6323.
- [54] F. Liu, J. Zhu, Y.F. Xu, L. Zhou, Y. Li, L.H. Hu, J.X. Yao, S.Y. Dai, *Chem. Commun.* 51 (2015) 8108-8111.
- [55] R.H. Zhang, S. Cho, D.G. Lim, X.Y. Hu, E.A. Stach, C.A. Handwerker, R. Agrawal, *Chem. Commun.* 52 (2016) 5007-5010.
- [56] X. Zhao, M.X. Lu, M.J. Koeper, R. Agrawal, *J. Mater. Chem. A* 4 (2016) 7390-7397.
- [57] F. Wang, D.D. Yang, Y.Y. Liao, Z.J. Ma, B. Hu, Y.Q. Wang, W.W. Xiong, X.Y. Huang, *Inorg. Chem.* 59 (2020) 2337-2347.
- [58] G.M. Sheldrick, *Acta Crystallogr. Sect. C* 71 (2015) 3-8.
- [59] J.N. Zhu, X.Q. Zhu, F.F. Cheng, P. Li, F. Wang, Y.W. Xiao, W.W. Xiong, *Appl. Catal. B: Environ.* 256 (2019) 117830.
- [60] W.W. Xiong, E.U. Athresh, Y.T. Ng, J.F. Ding, T. Wu, Q.C. Zhang, *J. Am. Chem. Soc.* 135 (2013) 1256-1259.
- [61] W.W. Xiong, J.W. Miao, K.Q. Ye, Y. Wang, B. Liu, Q.C. Zhang, *Angew. Chem. -Int. Ed.* 54 (2015) 546-550.
- [62] W.W. Xiong, Q.C. Zhang, *Angew. Chem. -Int. Ed.* 54 (2015) 11616-11623.
- [63] D.D. Yang, W. Li, W.W. Xiong, J.R. Li, X.Y. Huang, *Dalton Trans.* 47 (2018) 5977-5984.
- [64] D.D. Yang, Y. Song, B. Zhang, N.N. Shen, G.L. Xu, W.W. Xiong, X.Y. Huang, *Cryst. Growth Des.* 18 (2018) 3255-3262.
- [65] T. Cai, J.N. Zhu, F.F. Cheng, P. Li, W. Li, M.Y. Zhao, W.W. Xiong, *Inorg. Chim. Acta* 484 (2019) 214-218.
- [66] M.A. Pell, J.A. Ibers, *Chem. Ber. Recl.* 130 (1997) 1-8.
- [67] H. Li, C.D. Malliakas, J.A. Peters, Z.F. Liu, J. Im, H. Jin, C.D. Morris, L.D. Zhao, B.W. Wessels, A.J. Freeman, M.G. Kanatzidis, *Chem. Mater.* 25 (2013) 2089-2099.
- [68] H. Lin, J.N. Shen, L. Chen, L.M. Wu, *Inorg. Chem.* 52 (2013) 10726-10728.
- [69] W.W. Xiong, P.Z. Li, T.H. Zhou, Y.L. Zhao, R. Xu, Q.C. Zhang, *J. Solid State Chem.* 204 (2013) 86-90.
- [70] C.F. Du, J.R. Li, M.L. Feng, G.D. Zou, N.N. Shen, X.Y. Huang, *Dalton Trans.* 44 (2015) 7364-7372.
- [71] H.L. Li, J. Kim, T.L. Groy, M.O. Keeffe, O.M. Yaghi, *J. Am. Chem. Soc.* 123 (2001) 4867-4868.
- [72] C.Y. Chen, C.C. Ou, H.F. Huang, J.H. Cheng, C.S. Yang, *Inorg. Chem. Commun.* 14 (2011) 1004-1009.

Figure Captions

Scheme 1. Schematic illustration of synthetic procedures for compounds **1-3**.

Figure 1. Mapping images of compounds **1-3**.

Figure 2. (a) $[\text{In}_{2.6}\text{Sn}_{1.4}\text{Se}_6\text{S}_2]_n^{2.6n-}$ anionic layer of compound **1**. (b) Structure packing diagram of compound **1** viewed along the *a*-axis.

Figure 3. (a) $[\text{In}_{2.8}\text{Sn}_{1.2}\text{Se}_6\text{S}_2]_n^{2.8n-}$ anionic layer of compound **2**. (b) Structure packing diagram of compound **2** viewed along the *c*-axis. H atoms are omitted for clarity.

Figure 4. (a) $[\text{InGe}_4\text{S}_{11}(\text{SH})_2(\text{OH})]^{6-}$ discrete cluster of compound **3**. (b) Structure packing diagram of compound **3** viewed along the *b*-axis, H atoms are omitted for clarity.

Figure 5. Solid state optical absorption spectra of compounds **1-3**.

Figure 6. TG curves of **1-3** at a heating rate of 10 °C min⁻¹ from 30 to 800 °C in a N₂ atmosphere.

Figure 7. (a) Vis spectra of RhB aqueous solutions at different catalytic reaction times. (b) Removal efficiency of RhB by compound **1**.

Table 1. Crystallographic data and structure refinements for compounds **1-3**

	1	2	3
Chemical formula	C _{10.4} H _{31.2} N _{2.6} S ₂ Se ₆ In _{2.6} Sn _{1.4}	C _{13.2} H _{35.6} N _{4.8} S ₂ Se ₆ In _{2.8} Sn _{1.2}	C ₁₂ H ₄₅ N ₈ S ₁₃ InGe ₄ O
Formula mass	1195.39	1264.49	1139.76
Crystal system	Tetragonal	Orthorhombic	Orthorhombic
Space group	<i>P4₂/nmc</i>	<i>Pna2₁</i>	<i>Pnma</i>
<i>a</i> /Å	7.8752(3)	13.3741(14)	21.2157(9)
<i>b</i> /Å	7.8752(3)	28.778(2)	11.3247(5)
<i>c</i> /Å	25.283(2)	8.0083(7)	15.6853(7)
<i>α</i> /°	90	90	90
<i>β</i> /°	90	90	90
<i>γ</i> /°	90	90	90
<i>V</i> /Å ³	1568.00(18)	3082.2(5)	3768.6(3)
<i>Z</i>	2	4	4
Measured refls.	7753	19549	14644
Independent refls.	973	6722	4302
<i>R</i> _{int}	0.1113	0.1062	0.0876
<i>GOF</i>	1.003	1.039	1.058
<i>R</i> ₁ (<i>I</i> > 2σ(<i>I</i>))	0.0630	0.0813	0.0866
<i>wR</i> (<i>F</i> ₂) (<i>I</i> > 2σ(<i>I</i>))	0.1705	0.1383	0.2165

Scheme 1

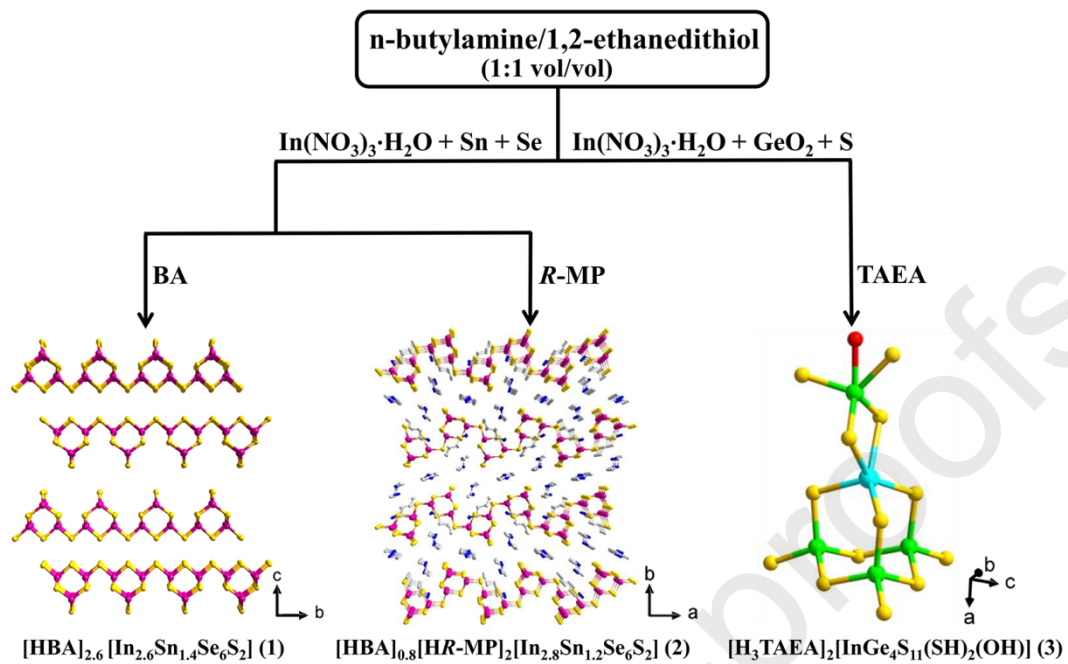


Figure 1.

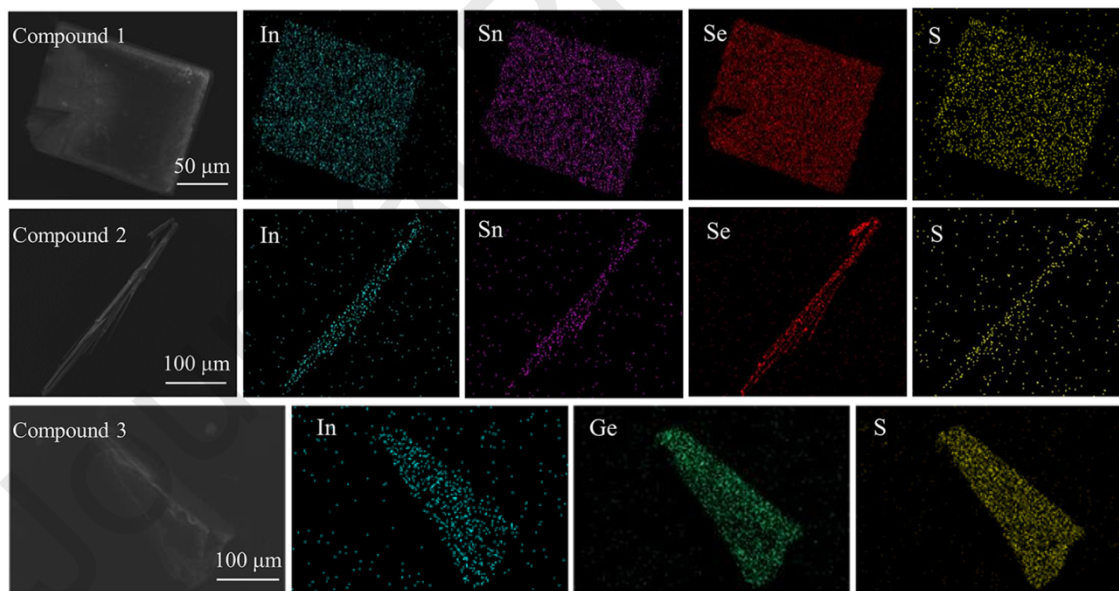


Figure 2.

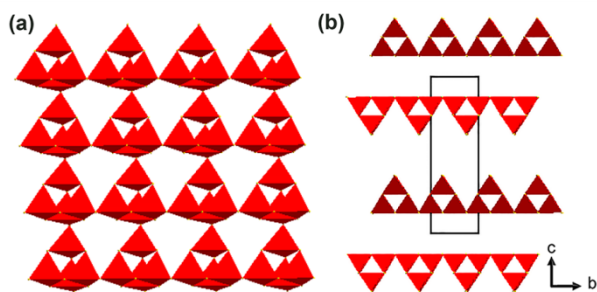


Figure 3.

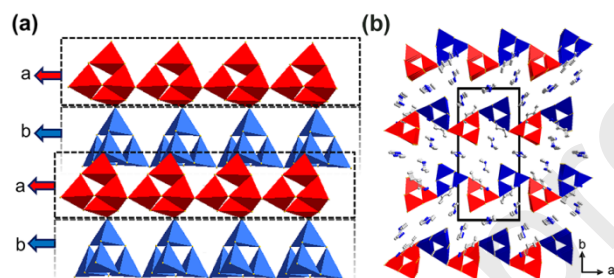


Figure 4.

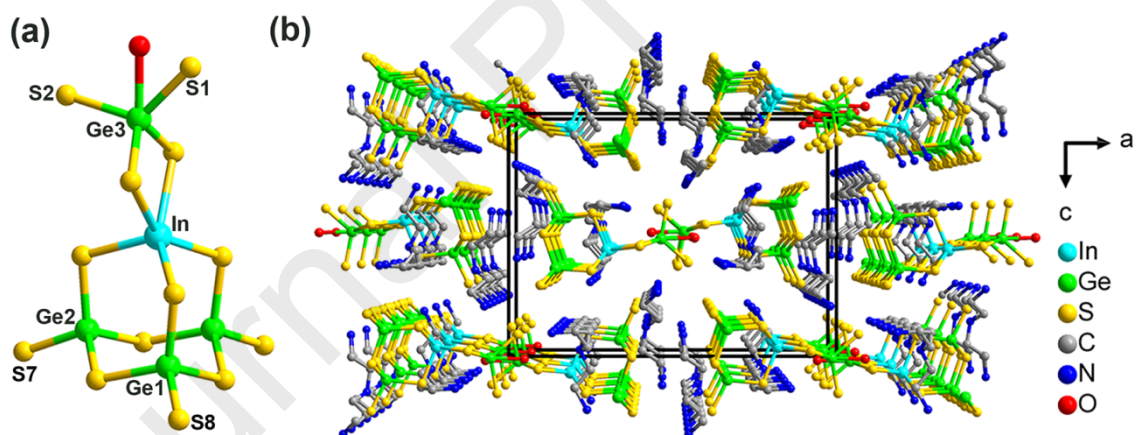


Figure 5.

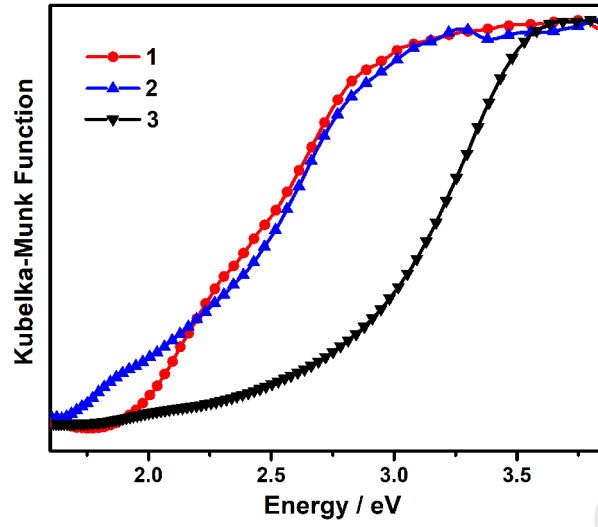


Figure 6.

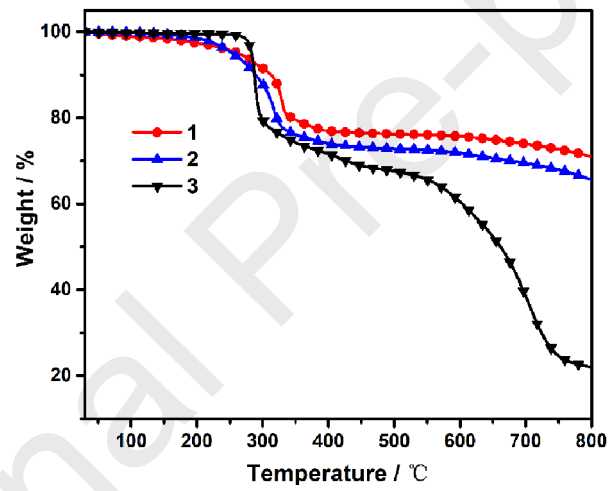
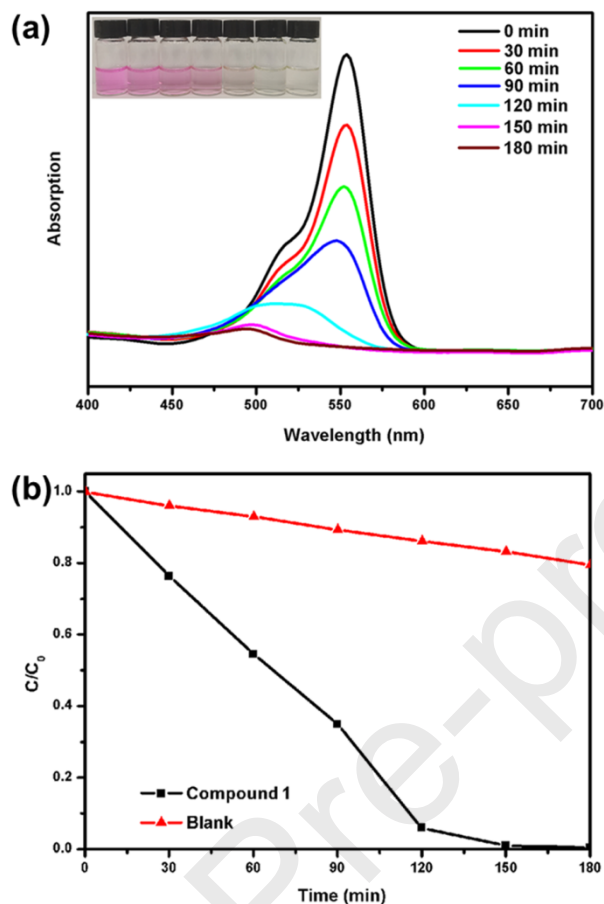


Figure 7.



CRedit author statement:

Ji-Ming Yu: Conceptualization, Writing - Original Draft. **Ting Cai:** Methodology, Investigation.

Zhong-Jie Ma: Visualization. **Fei Wang:** Data curation. **Huan Wang:** Data curation. **Ji-Peng Yu:**

Data curation. **Lu-Lu Xiao:** Data curation. **Fang-Fang Cheng:** Writing - Review & Editing, Project

administration. **Wei-Wei Xiong:** Supervision, Writing - Review & Editing.

Declaration of interests

The authors declare that they have no known competing financial interests or personal relationships that could have appeared to influence the work reported in this paper.

The authors declare the following financial interests/personal relationships which may be considered as potential competing interests:

Highlight:

1. Three new heterometallic chalcogenides were synthesized in a thiol-amine solvent mixture.
2. The thiol-amine solvent mixture was crucial to the crystal growths of these compounds.

Title: Using thiol-amine solvent mixture to prepare main group heterometallic chalcogenides

Authors: Ji-Ming Yu^a, Ting Cai^a, Zhong-Jie Ma^a, Fei Wang^a, Huan Wang^a, Ji-Peng Yu^a, Lu-Lu Xiao^a, Fang-Fang Cheng^{b,*}, Wei-Wei Xiong^{a,*}

